Wind and Structures, Vol. 16, No. 4 (2013) 373-391
DOI: http://dx.doi.org/10.12989/was.2013.16.4.373

Wind-induced response and loads for the Confederation Bridge. Part I: on-site monitoring data

Bilal Bakht *1, J. Peter C. King[2] and F.M. Bartlett[3]

[1] *Ministry of Transportation and Infrastructure, KAMLOOPS BC, Canada*
[2] *Boundary Layer Wind Tunnel Laboratory, University of Western Ontario, London ON, Canada*
[3] *Department of Civil and Environmental Engineering, University of Western Ontario, London ON, Canada*

(Received September 7, 2011, Revised March 25, 2012, Accepted May 17, 2012)

Abstract. This is the first of two companion papers that analyse ten years of on-site monitoring data for the Confederation Bridge to determine the validity of the original wind speeds and wind loads predicted in 1994 when the bridge was being designed. The check of the original design values is warranted because the design wind speed at the middle of Northumberland Strait was derived from data collected at shore-based weather stations, and the design wind loads were based on tests of section and full-aeroelastic models in the wind tunnel. This first paper uses wind, tilt, and acceleration monitoring data to determine the static and dynamic responses of the bridge, which are then used in the second paper to derive the static and dynamic wind loads. It is shown that the design ten-minute mean wind speed with a 100-year return period is 1.5% less than the 1994 design value, and that the bridge has been subjected to this design event once on November 7, 2001. The dynamic characteristics of the instrumented spans of the bridge including frequencies, mode shapes and damping are in good agreement with published values reported by others. The on-site monitoring data show bridge response to be that of turbulent buffeting which is consistent with the response predicted at the design stage.

Keywords: full-scale; long-span; bridge damping; design wind speed; bridge acceleration; spectral analysis; mode shape; frequency; structural health monitoring

1. Background

The Confederation Bridge, shown in Fig. 1, is a 13 km long precast concrete structure that was constructed between 1993 and 1997 connecting Prince Edward Island and New Brunswick across the Northumberland Strait. The main superstructure is comprised of 43 – 250 m spans that alternate between rigid frame and cantilever/drop-in span arrangements. A detailed description of the bridge, including its design and construction, has been presented by Tadros (1997). Wind studies were conducted in the early '90s at the Boundary Layer Wind Tunnel Laboratory (BLWTL) to predict the 100-year wind speed and associated wind loads for the design of the bridge. Traditionally, section models are used to obtain wind loading information; however, the variable depth of the Confederation Bridge deck girder cross-section prevented this approach from being

*Corresponding author, Dr., E-mail: Bilal.Bakht@gov.bc.ca

used. Consequently, a new methodology was developed for the derivation of dynamic wind loads using a full-aeroelastic model of the Confederation Bridge (King *et al*. 1994, King *et al*. 1995).

Recognising the scale and uniqueness of the structure, the owners of the bridge, Strait Crossing Development Inc. and Public Works and Government Services Canada, jointly implemented a comprehensive bridge monitoring programme to capture and archive the interaction of the bridge with its environment. The complex instrumentation system shown in Fig. 2, including accelerometers, tiltmeters and anemometers, was installed along a one-kilometre section of the bridge between Piers 30 and 33, on the western approach to the central "navigation" spans. The dynamic motions of the bridge are captured by 76 accelerometers. Tiltmeters at Piers 31 and 32 measure pier rotations in the transverse and longitudinal directions. Anemometers mounted atop five lamp standards along the bridge, shown in Fig. 1, record wind speed and direction data that are archived as statistical summaries and time histories. Six High Speed Data Loggers (HSDLs) (Montreuil 1999a) and nine Slow Speed Data Loggers (SSDLs) (Montreuil 1999b) are connected by a fibre-optic network to a central computer system that transmits the data through the internet to various research institutions for archiving and analysis (Cheung *et al*. 1997). The bridge monitoring system has been operational, with interruptions, since 1998, providing statistical and time history data for different wind, ice, and traffic conditions.

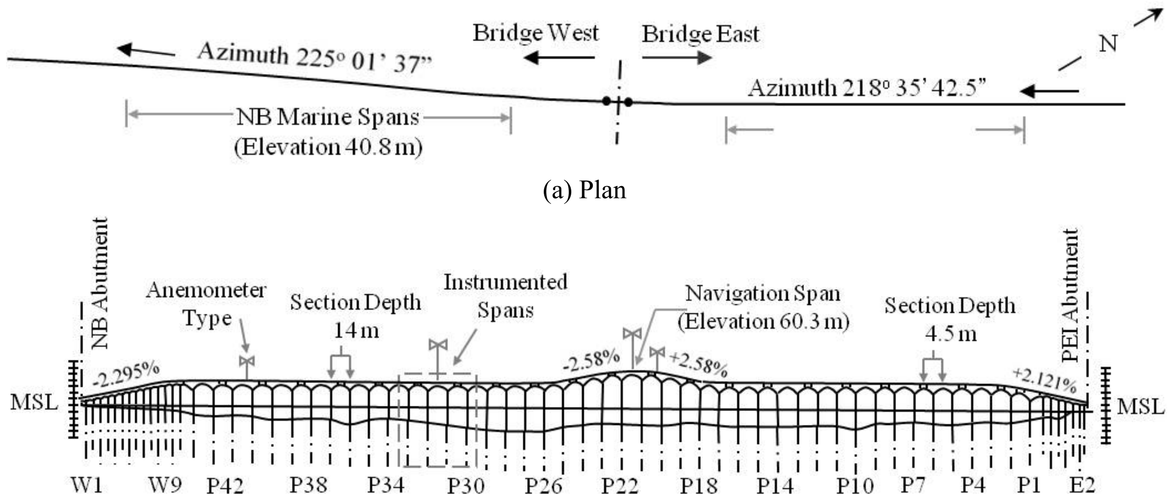

(a) Plan

(b) Elevation

Type	Location Along Span	Side of Bridge	Elevation	Count
Bridge Operations	41.67 m West of Pier 20	North	61 m	1
Bridge Operations	83.33 m West of Pier 20	South	60 m	1
Environment Canada	Midspan Pier 21 – 22	North	73 m	1
Primary for Research	Midspan Pier 31 – 32	North	54 m	2
Bridge Operations	41.67 m West of Pier 41	North	47 m	1

(c) Description of bridge anemometers

Fig. 1 Bridge Plan and Elevation Showing Anemometer Locations (adapted after King *et al*. 1994)

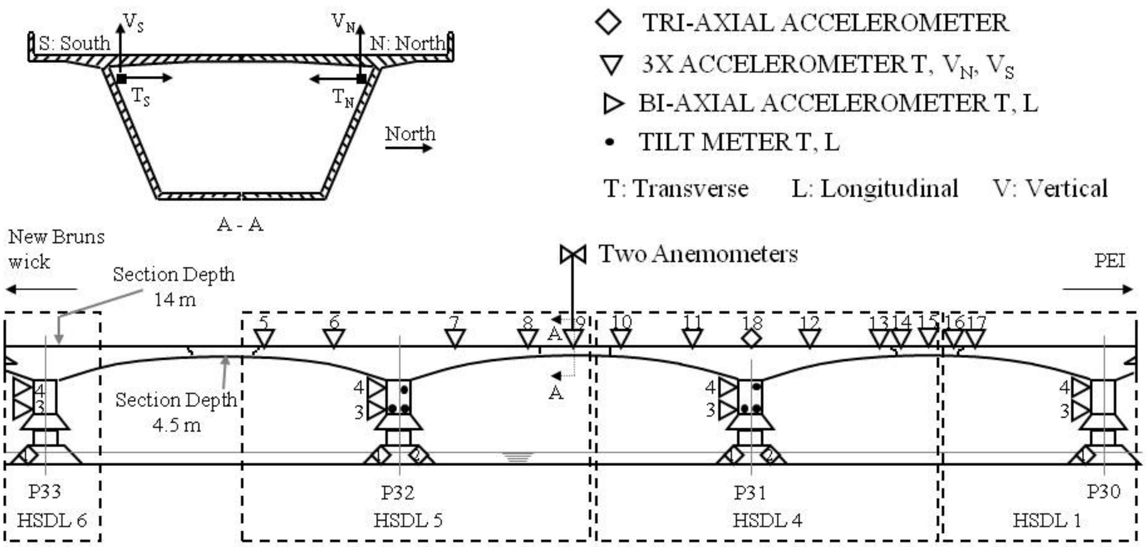

Fig. 2 Accelerometer and Ttiltmeter Locations for Static and Dynamic Monitoring (adapted from Montreuil 1999a)

Strait Crossing Bridge Limited provided the BLWTL with on-site monitoring data obtained from 1998 to 2007 to compare the actual bridge response with that derived at the design stage. Using a new approach, the research reported in this paper uses these on-site monitoring data to derive wind loads that will be compared to loads adopted for the design of the bridge in the early '90s based on wind studies (King *et al*. 1994, King *et al*. 1995). The full-scale bridge response has been presented by others (Londoño 2006, Lau *et al.* 2004 and Naumoski *et al*. 2002, 2004), however, this will be the first time that wind loads will have been derived from the observed response of the full-scale structure, and the first time that the validity of wind loadings determined from aeroelastic model studies will be investigated. The analysis of the data and the derivation of wind loads will be presented in two companion papers. The first paper will present analysis of the data from the on-site monitoring programme and the second paper will present the derivation of wind loads using these data.

2. Introduction

An analysis of the available surface wind records in 1994 indicated that the Borden and Cape Tormentine ferry terminals had the best information representative of conditions at the bridge site and so wind records from these sites were used to develop statistical models of the wind climate (King *et al.* 1994). Transferring these data to the future bridge location was challenging because these two sites are 14.5 km apart, and so the accuracy of the predicted wind speeds at the marine and navigation spans, located in the middle of the strait as shown in Fig. 1, was uncertain. The 100-year ten-minute mean wind speed at 10 m above Mean Sea Level (MSL) was predicted to be 29.6 m/s. The corresponding mean wind speeds at the deck elevation of the marine and navigation spans, at 40.8 and 60.3 m above MSL, respectively, were 35.4 m/s and 34.1 m/s, respectively.

These design wind speeds became the basis for all subsequent wind tunnel investigations (King *et al*. 1994).

It was unclear whether the bridge had been exposed to the 100-year return period wind speed during its first ten years of operation. Analysis of wind data by Naumoski *et al*. (2004) suggested that the specified design wind speed was exceeded once in November 2001. Their maximum reported wind speed of 43 m/s would correspond to a return period approaching 1000 years (King et al. 1994) and so seems excessive. Thus, it is imperative to validate the 100-year wind speed specified for the design of the Confederation Bridge using on-site monitoring data before it could be used for the derivation of wind loads.

Another necessary step in the derivation of wind loads is to accurately quantify the static and dynamic responses of the full-scale structure due to turbulent buffeting in strong wind conditions. The occurrence of instabilities such as galloping, vortex shedding and flutter should also be investigated. Section model tests carried out in 1994 (King *et al*.) for different depths of the bridge section showed vortex shedding; however, tests of a full-aeroelastic model, which replicates the geometry, stiffness and mass properties of the entire bridge, did not show instabilities up to full-scale wind speeds of 60 m/s given a low structural damping of 0.63%. The typical response predicted was instead characterized by turbulent buffeting. These wind tunnel predictions, however, need to be validated using the prototype response. In addition, the mode shapes, frequencies, and damping must be determined. This will be accomplished using on-site monitoring data from anemometers, accelerometers and tiltmeters recorded between 1998 and 2006. Much of the tiltmeter data has been analysed by a research group at the University of Calgary, headed by Brown (2007), to obtain ice forces on the piers of the instrumented spans. The analysis of these data to quantify the wind component of pier tilt has been well documented (e.g., Bruce and Croasdale 2001), and will be used in the companion paper to derive the static wind force coefficients.

The original 1994 wind tunnel tests were based on natural frequencies and mode shapes determined from numerical models of the prototype provided by the designers (JMS 1995). These numerical models idealized three spans of the bridge representing typical marine and navigation spans using appropriate pier heights and assumed material properties. Frequencies reported by Londoño (2006) are for the instrumented marine spans, which have different pier heights than the typical marine and navigation spans, and are therefore different from the values assumed at the design stage. These values need to be confirmed as they are required to derive wind loads in the companion paper.

Very little was known about the prototype damping at the design stage and so a low value of 0.13% of critical was originally used to identify instabilities and a value of 0.63% of critical, considered to be conservative for prestressed concrete structures, was used for the remaining wind tunnel tests (King *et al*. 1994, King *et al*. 1995). The damping estimated by Londoño (2006) and particularly by Brown and Bruce (1997) are significantly higher than these values. Given this lack of consensus, further investigation is necessary to accurately estimate the bridge damping. These damping estimates of the full-scale structure are necessary to determine the equivalent full-scale wind loads developed from various wind tunnel investigations.

This first paper addresses these issues and uses on-site monitoring data to determine the 100-year design wind speed, full-scale bridge response and dynamic properties (frequencies, mode shapes and damping) of the Confederation Bridge. The specific objectives are:

1. To determine the 100-year wind speed at the marine span deck elevation of 40.8 m and compare it to the originally specified 100-year design wind speed of 34.1 m/s (King *et al*.

1994).

2. To investigate the accuracy of the claim by Naumoski *et al*. (2004) that the bridge experienced wind speeds significantly greater than the specified 100-year speed during the November 2001 storm.
3. To quantify dynamic properties of the Confederation Bridge, i.e., natural frequencies, mode shapes and damping for comparison with the values reported by others.
4. To modify an existing numerical model of the Confederation Bridge and validate it with the full-scale measurements of the mode shapes and frequencies.
5. To derive the dynamic bridge response, in the form of RMS normalized modal displacements that will be used in the companion paper to derive the dynamic wind loads.
6. To investigate the occurrence of instabilities such as galloping, vortex shedding, and flutter to confirm the predicted bridge response as primarily that due to turbulent buffeting.

3. Analysis of the 1998 – 2007 wind data

The harsh marine environment of the Northumberland Strait has caused anemometers to fail intermittently, which has affected the overall continuity and availability of the wind speed and direction data. The Handar (ultrasonic) anemometer, used primarily for research (Bakht 2010), was initially installed at 12.85 m above the bridge deck atop a light standard midway between Pier 31 and Pier 32, as shown in Fig. 1, to monitor wind speeds and directions. In 2007 an R.M. Young Propeller-type anemometer was installed beside the functioning Handar anemometer as a backup but has only provided data since November 2007. Both anemometers are scanned at 1 Hz sampling frequency by the Slow Speed Data Logger 8 located at Pier 31 (Fig. 1(b)) which records maximum, average, minimum and RMS statistics for wind speed and azimuth every ten minutes. When the wind speed exceeds 15 m/s, time histories of the wind speed and azimuth are also digitized at one-second intervals (Bakht 2010).

Two other anemometers used for bridge operations are approximately 6 m above the bridge deck 42 m west of Pier 20 and 42 m west of Pier 41 as shown in Fig. 1(b). These are cup-and-vane anemometers that collect six-minute mean and maximum wind speeds and azimuths using a 16-point compass. Both are located on the north side of the bridge. A third cup-and-vane anemometer was installed in 2008 on the south side of the bridge, 82 m west of Pier 20 (Fig. 1), to provide additional information relevant for winds from the south. These are well-maintained instruments with reliable service histories due to their importance to bridge operations.

3.1 Data analysis

Analysis of the data from the Handar anemometer revealed that the anemometer or data logger malfunctioned approximately 40% to 50% of the time (Bakht 2010). To develop estimates of extreme winds with this incomplete dataset it was necessary to considerably supplement the Handar data with data from another source. Data from the most reliable anemometer, located 2.83 km east of the Handar anemometer and 41.67 m west of Pier 20 on the north side of the bridge, as shown in Fig. 1, were used for this purpose. As described earlier, the Pier 20 anemometer records six-minute mean and maximum wind speeds and wind directions on a 16-point compass, and has a reliability of almost 100%. The Pier 20 data were adjusted to be compatible with the Pier 31-32 data: for example, the former report wind azimuth with respect to True North and the latter uses a datum of Bridge North that is normal to the bridge axis. Other subtle factors can cause the readings to be different, as discussed in detail by Bakht (2010), including the different averaging time, different elevation with respect to the bridge deck at MSL, and different location with respect to midspan.

3.2 Maximum wind speed recorded between January 1998 and June 2007

Inspection of the complete dataset (January 1998 – June 2007) indicates that the maximum ten-minute mean wind speed was 31.3 m/s, normal to the bridge axis, and occurred at 21:00 on 7th November 2001. This recorded value reflects the wind speed at the 54 m elevation of the anemometer. Assuming an open sea exposure, this is equivalent to a mean wind speed of 30.5 m/s at the deck elevation of 40.8 m (ESDU 1993). The originally specified design wind speed of 34.1 m/s at this elevation is a ten-minute mean wind speed considering winds from all directions (King et al. 1994). If only winds normal to the bridge axis are considered, a corresponding design wind speed of 30.5 m/s at the deck level was suggested (King *et al*. 1994). Thus this 20-minute interval during the November 2001 storm represents the only wind event in ten years, from 1998 to 2007, when the recorded 10-minute mean wind speed approached the specified design wind speed for the Confederation Bridge. The bridge is actually designed to resist a factored wind load that is 1.9 times the specified wind load (MacGregor *et al*. 1997) and therefore corresponds to a wind speed that is 38% greater than the specified design wind speed.

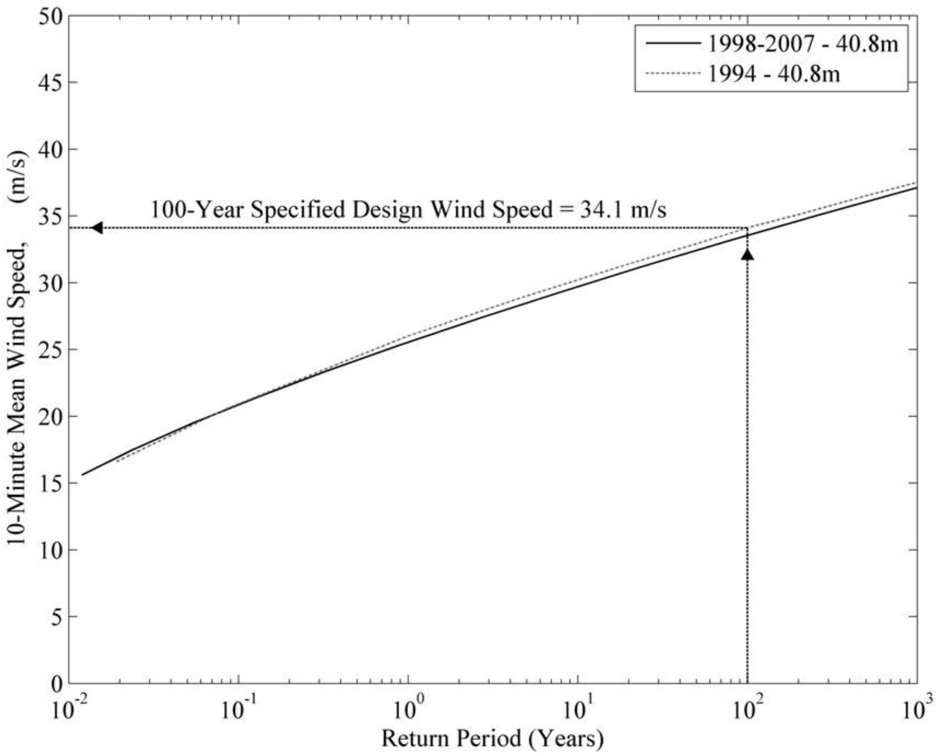

Fig. 3 Design Wind Speed for Various Return Periods Computed Using 1998-2007 On-Site Monitoring Data and Pre- 1994 Borden & Cape Tormentine Data

Naumoski *et al*. (2004) report that the Confederation Bridge was subjected to wind speeds that were significantly greater than the design wind speed during the November 2001 storm. The maximum wind speed they report, 43 m/s (155 km/h) at the Pier 20 anemometer, is a three-second gust speed at 61 m above MSL. The severity of this reading is exaggerated because the difference between the three-second gust and ten-minute mean wind speed, which is approximately a factor of 1.44 in an open exposure (ASCE 7 2005), is not accounted for. The wind speed recorded at 61 m is also not corrected to an equivalent value at the bridge deck elevation of 40.8 m, an additional factor of 1.025 (ESDU 1993). Adjusting the reported value of 43 m/s by these factors results in a corresponding mean wind speed of 29.1 m/s, which is close to the observed value of 30.5 m/s.

Fig. 3 compares the ten-minute mean wind speeds for various return periods computed using the on-site monitoring data recorded between 1998 and 2007, corrected to the 40.8 m deck elevation, with the values predicted at the design stage using data from the weather stations in Borden and Cape Tormentine (King *et al*. 1994). The crossing rate for different wind speed intervals integrated over all wind directions was determined from the 1998-2007 data and fitted using bi-modal Weibull Distribution (Xu 2008) and Rice's Theory extended by Davenport (1964, 1977). The return period is the inverse of the annual probability of exceedance for a given wind speed interval. The figure shows the ten-minute mean wind speed for a 100-year return period based on the on-site monitoring data is 33.6 m/s at the deck elevation. This value is in remarkably close agreement with the originally specified design wind speed of 34.1 m/s.

4. Available accelerometer data

Fig. 2 shows the locations of accelerometers and tiltmeters attached to the bridge between Piers 30 and 33 to facilitate the on-site monitoring programme that was initiated in 1998. The instruments are scanned by High Speed Data Loggers 1, 4, 5, and 6 represented as dashed rectangles in the figure. The calibration factors for the accelerometers and tiltmeters and the specifications for the data loggers are reported by Montreuil (1999a).

The accelerometer data are stored as statistical summaries and may also be stored as time histories. The statistical summaries are 15-second mean and Root Mean Square (RMS) records, which are further averaged over ten-minute intervals and so are readily correlated with the ten-minute wind statistical summaries presented earlier. The ten-minute accelerometer time history records, sampled at a frequency of 125 Hz by the HSDLs are recorded when the ten-minute mean wind speed exceeds 15 m/s. The time history datasets obtained from 1998 to 2002 are only 30 or 90 seconds in duration, and so are too short to accurately characterize the acceleration power spectrum: the bridge is designed for a ten-minute mean wind speed as described earlier and so a minimum record duration of ten minutes is required for spectral analysis. Thus only time history records obtained since 2003 could be used for the spectral analysis. On-site monitoring accelerometer data, whether in the form of statistical summaries or time histories, were categorized based on wind speeds and azimuths defined using a 16-point compass.

5. Frequencies and mode shapes

Table 1 compares full-scale observed frequencies for the first ten natural modes of vibration, derived from power spectra (Davenport and King 1984, Davenport 1988) in the present study, with

Table 1 Comparison of Frequencies Computed from On-Site Monitoring Data and Predicted Using Numerical Model for the Marine Span Between Piers 31 and 32

Frequencies Computed from On-Site Monitoring						Numerical Model Frequencies	
		Proesent study		Londoño 2006		Beam element model (Londoño 2006)	Modified beam element model (ALGOR) (Bakht 2010)
Mode	Type	Mean	Variability	Mean	Variability		
		(Hz)	(% of Mean)	(Hz)	(% of Mean)	E_c = 43 GPa	E_c = 43 GPa
1	TS1	0.34	4	0.34 (-1%)	16	0.31 (-10%)	0.35 (+2%)
2	TS2	0.49	1	0.47 (-3%)	5	0.51 (+5%)	0.50 (+2%)
3	VA1	0.57	1	0.57 (0%)	19	0.52 (-9%)	0.50(-13%)
4	VS1	0.68	1	0.68 (0%)	9	0.69 (+2%)	0.68 (0%)
5	TA2	0.91	2	0.89 (-3%)	5	0.93 (+2%)	0.88 (-4%)
6	VS2	0.94	1	0.92 (-2%)	7	0.88 (-7%)	0.89 (-5%)
7	TS3	1.33	2	1.31 (-2%)	1	1.33 (0%)	1.31 (-1%)
8	VA2	1.81	1	1.81 (0%)	5	1.78 (-2%)	1.87 (+3%)
9	VS3	2.81	1	2.88 (+3%)	4	-	2.87 (+2%)
10	VA3	-	-	3.79	5	3.42	3.58

Note: values in brackets are percentage difference with respect to mean frequencies computed from on-site monitoring data in the present study

the frequencies observed and predicted by Londoño (2006). Mode shapes for the first seven fundamental frequencies are shown in Fig. 4. Also shown are frequencies predicted by Bakht (2010) using the numerical model developed for a typical marine span by JMS (1995) that was modified to reflect the properties of the marine span between Piers 31 and 32. The mode type designation uses the symbols T and V for transverse and vertical modes, respectively, and S and A for symmetric and asymmetric mode shapes. Thus, for example, TS2 is the second transverse symmetric mode.

As shown in Table 1, the frequencies computed from the on-site monitoring data in the present study have a variability of less than 2% of the mean value for Modes 2 through 8 whereas the variability of Mode 1 is roughly 4% of the mean. The frequencies computed from the on-site accelerometer monitoring data by Londoño (2006), have variabilities less than 10% of the mean value for all modes except TS1 and VA1, which have variabilities less than 20% of the mean value. The variabilities in the present study are markedly less than those reported by Londoño because only accelerometer data for wind speeds greater than 15 m/s were used to derive frequencies whereas Londoño is believed to have used data representing various loading conditions including severe wind events, heavy traffic events and ambient traffic conditions with or without ice loading present (Londoño 2006). Nevertheless, the mean values of Londoño's observed frequencies are within 3% of the mean values of the observed frequencies derived in the present investigation. The numerical beam-element model frequencies reported by Londoño, are also shown in Table 1, and are within 10% of those computed from the full-scale monitoring data in the present investigation. The model frequencies determined using the modified ALGOR model in the present study are generally within 5% of the mean frequencies computed from the full-scale monitoring data. The exception is Mode VA1, where the numerical model value of 0.5 Hz is 13% less than the full-scale monitoring-based value of 0.57 Hz. At the present time, no explanation has been found for this discrepancy.

Fig. 4 shows a comparison of the mode shapes extracted by Londoño from the accelerometer time histories, shown in open circles, with the mode shapes determined from the modified ALGOR model, shown in solid lines. These mode shapes correspond to the fundamental bridge frequencies having values less than 1 Hz and so are important to characterize the wind-induced response. The horizontal axis in each figure is the horizontal distance from the midspan between Piers 31 and 32, so $x = -125$ m at Pier 31, 125 m at Pier 32 and +/– 220 m at the tips of the cantilevers. The mode shapes from both studies are in good agreement for the frequencies of interest. The fit to transverse asymmetric mode TA2 is not ideal at the points where the cantilever tip connects to the drop-in span at x = +/– 220 m but this is not critical. Thus the mean frequencies and numerical mode shapes computed in the present study will be used to compute dynamic wind loads in the companion paper.

6. Dynamic bridge response

The wind-induced bridge dynamic response can be expressed in terms of several different structural actions including forces, bending moments, stresses, displacements or accelerations. Davenport (1988) has shown that the total dynamic response, R_{t_d}, can be expressed as

$$R_{t_d} = \sqrt{R_b^2 + \sum_j R_{r_j}^2} \tag{1}$$

where R_b^2 is the mean square non-resonant background response varying slowly and irregularly with time; and $R_{r_j}^2$ are the mean square resonant responses, also called modal dynamic responses, due to oscillations with varying amplitudes in the j^{th} natural vibration mode $j = 1, 2, \ldots n$.

Investigation of the acceleration power spectra at different bridge locations has shown that the fundamental modes of vibration contain more than 95% of the energy and the contribution of non-resonant background response is less than 5% (Bakht 2010). Given this absence of non-resonant background response, i.e., $R_b^2 \cong 0,$ Eq. (1) simplifies to

$$R_{t_d} \cong \sqrt{\sum_j R_{r_j}^2} \tag{2}$$

6.1 Ten-Minute duration accelerometer datasets

Fig. 5 shows ten-minute RMS accelerations in the transverse and vertical directions at: the midpoint of the continuous span, Accelerometer 9 on Fig. 2; the tip of the cantilever, Accelerometer 5 on Fig. 2; the quarter point of the continuous span, Accelerometer 7 on Fig. 2; and the midpoint of the drop-in span, Accelerometer 15 on Fig. 2. The RMS accelerations shown are the total dynamic responses, expressed by Eq. (2), caused by winds with azimuths within ± 11.25° of normal to the bridge axis. Large RMS accelerations at low wind speeds, occurring particularly at the two cantilever accelerometers in both transverse and vertical directions were examined for the

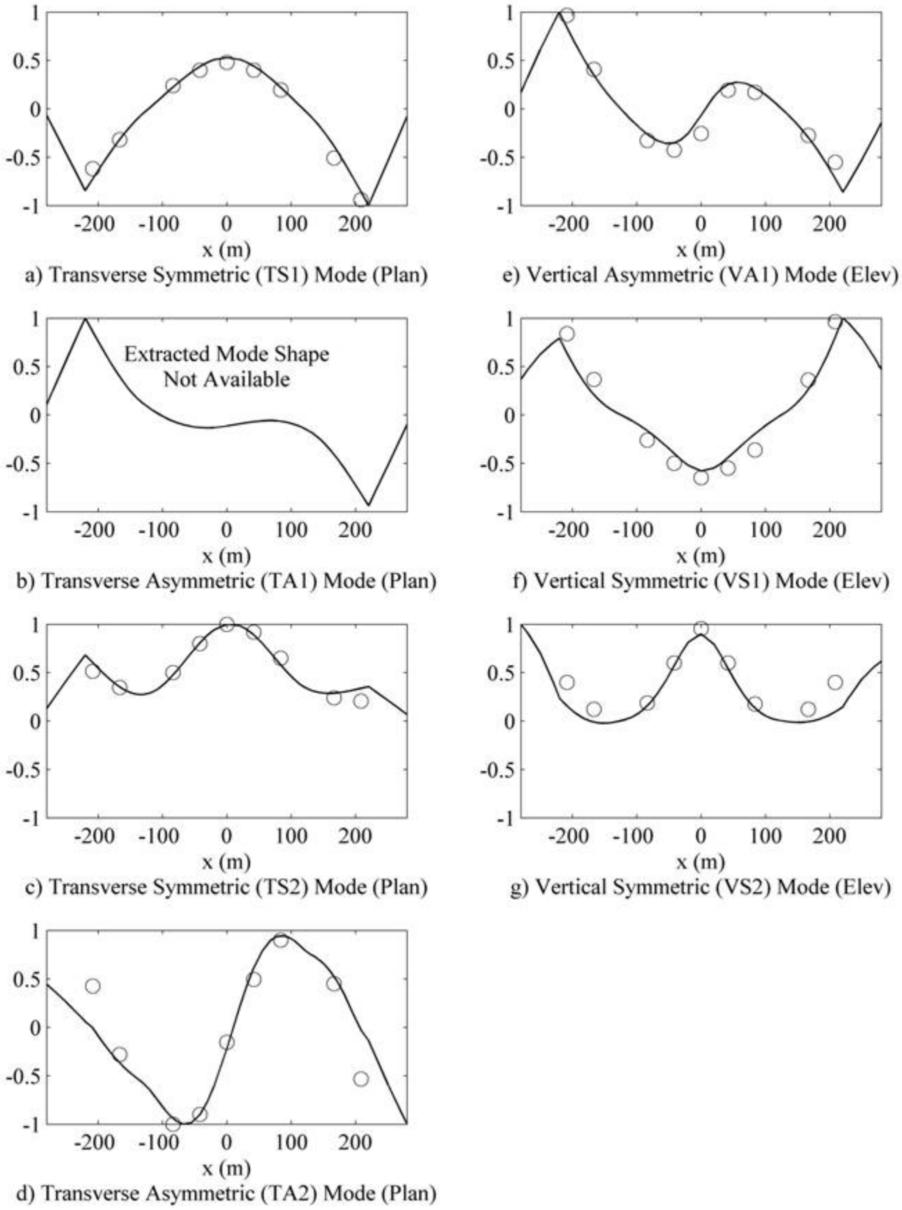

Fig. 4 Comparison of the Fundamental Modes of Vibration

signs of potential vortex shedding-induced vibration. In all cases the peak factors of the responses (i.e., the ratio of the peak to the RMS acceleration) were in the range of 3 to 5, which is typical of random response. Sinusoidal response as would be the case with vortex shedding excitation is typically characterized by low peak factors of the order of $\sqrt{2}$, which is the maximum/RMS of a sinusoidal signal. Therefore, it is believed that most of these events were related to heavy truck traffic and not wind loading. At wind speeds around 20 m/s, the wind-induced RMS accelerations

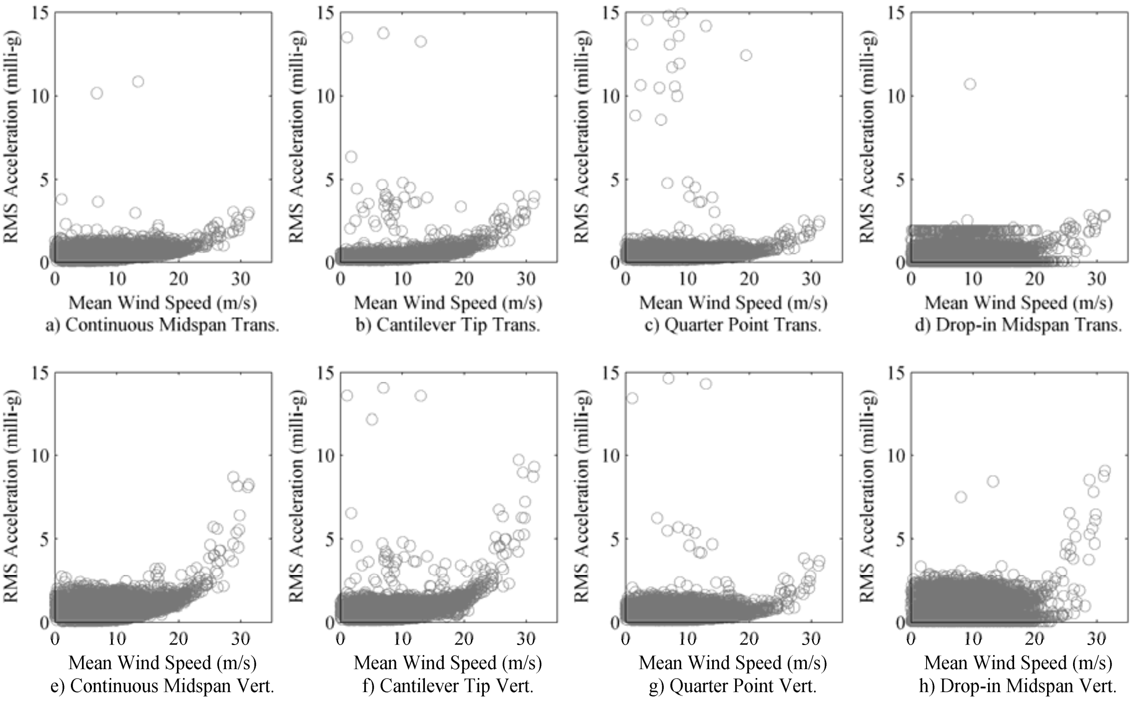

Fig. 5 Observed Ten-Minute RMS Accelerations – Total Dynamic Response

become more significant than those due to traffic. This is a typical buffeting response which confirms the response envisaged at the design stage (King *et al*. 1994).

King *et al*. (1994) performed wind tunnel tests of the Confederation Bridge models (section and full-aeroelastic) in the early '90s. The dynamic tests of the three uniform depth section models (4.5 m, 6.26 m and 11.86 m) were conducted under unrealistically low values of structural damping (0.15% of critical) which showed evidence of vortex shedding-induced vertical response. However, the amplitude of this response reduced markedly when the structural damping was increased through values of 0.15 to 0.26 to 0.5 and finally to 0.95%. At a value of 0.5%, the vortex shedding peak was completely eliminated, indicating that at levels which may be expected in full-scale vortex shedding induced response should not be anticipated. The full-aeroelastic model (constructed at a scale of 1:250) was tested with two structural damping values of 0.13% and 0.63 % of critical. Vortex shedding was not observed in either case. Galloping was prevalent in the model at a full scale mean hourly wind speed of 40 m/s with abnormally low damping (0.13%) but not with realistic damping. The authors carried-out extensive wind tunnel tests of a full-aeroelastic model of the Confederation Bridge in 2009 (Bakht 2010). Comments regarding the absence of vortex shedding induced response and galloping behaviour in abnormally low damping conditions are appropriate.

The cantilever tip experiences maximum RMS accelerations of approximately 5 and 10 milli-g in the transverse and vertical directions, respectively. The associated wind speed at the deck level (40.8 m) is 30.5 m/s, which also corresponds to the specified design wind speed for the Confederation Bridge (King *et al*. 1994, JMS 1995), and occurred during the November 2001 storm. Detailed analysis of the data from the on-site monitoring programme showed that a significant number of the accelerometers provide redundant information concerning the modal response of the bridge. Out of 76 accelerometers attached to the bridge, eight strategically placed accelerometers are sufficient to fully quantify wind-induced response.

The modal dynamic responses can be determined using these acceleration time histories. The steps involved in their derivation are as follows:

(i) Power spectra are derived (Davenport and King 1984, Davenport 1988) to identify spectral peaks for the fundamental modes of vibration. Figs. 6(a) and (b) show typical power spectra derived for a single ten-minute time history from the transverse accelerations at the mid- and quarter-point of the continuous span respectively. Fig. 6(c) shows power spectra derived from vertical accelerations at the midpoint of the continuous span. The spectral peaks shown in both figures correspond to the fundamental modes of vibration shown in Fig. 4 and the shaded peaks represent the locations for each mode where the maximum modal displacement occurs. In Fig. 6(a), the first symmetric and asymmetric modes, TS1 and TA1, are very close in frequency and are inseparable. The second asymmetric mode, TA2, is significant only at the quarter point of the continuous span, which is consistent with the large lateral deflection at x = -83.5 m for mode TA2 as shown in Fig. 4.

(ii) The spectral peaks at the locations of the maximum modal displacements are isolated using a band-pass filter and the resulting time histories are used to compute the modal RMS accelerations. Fig. 4 shows that the maximum modal displacements at the cantilever tip for the first transverse symmetric and asymmetric modes of vibration (i.e., TS1 and TA1). The maximum modal displacement for the second transverse symmetric mode, TS2, occurs at the middle of the continuous span and that for the second transverse asymmetric mode, TA2, at the quarter point of the continuous span.

Figs. 6(a) and (b) show that the spectral peaks corresponding to Modes TS1 and TA1 overlap and therefore cannot be easily isolated using a single band-pass filter. Consequently, the modal RMS accelerations for these two transverse modes were not estimated using this approach. This does not impact the analysis as it will be shown later that not all modes of vibration are necessary to characterize the modal response. For the second transverse symmetric and asymmetric modes of vibration, the corresponding spectral peaks are shown shaded between the lower and upper limits of the band pass filters in Figs. 6(a) and (b). The filtered time histories were used to compute the modal RMS accelerations for these two modes of vibration (Davenport 1988, King 2003).

Fig. 6(c) shows the spectral peak for Mode VS1 at the midpoint of the continuous span can be used to determine the RMS acceleration for this mode. Fig. 4 shows that the maximum modal displacement for Mode VS1 occurs at the cantilever tip. Therefore, the RMS acceleration computed from the spectral peak at the midpoint of the continuous span requires a modal correction to estimate the maximum RMS acceleration for this mode. This correction is determined as the ratio of the maximum modal displacement at the cantilever tip to the modal displacement at the midpoint of the continuous span. The second vertical symmetric mode, VS2, does not require this correction because the maximum modal displacement occurs at the midpoint of the continuous span. Thus the spectral peaks shown shaded in Fig. 6(c) were band-pass filtered and the resulting time histories were used to calculate the maximum modal RMS accelerations (Davenport 1988, King 2003). This step was repeated for the 2076 ten-minute time history datasets available in the database.

(iii) The maximum modal RMS accelerations and associated mean wind speeds are normalized with respect to the natural frequency of the mode and the width of the bridge. This makes the

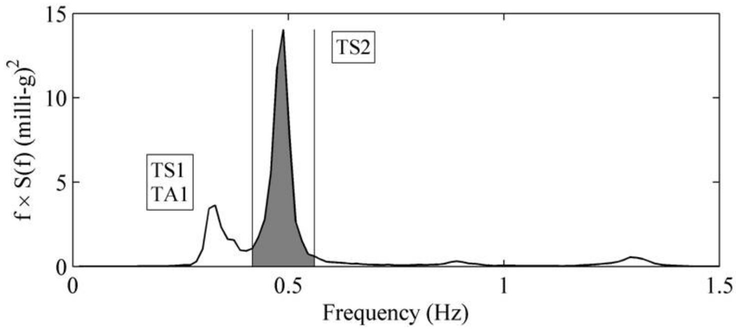

(a) Midpoint Continuous Span

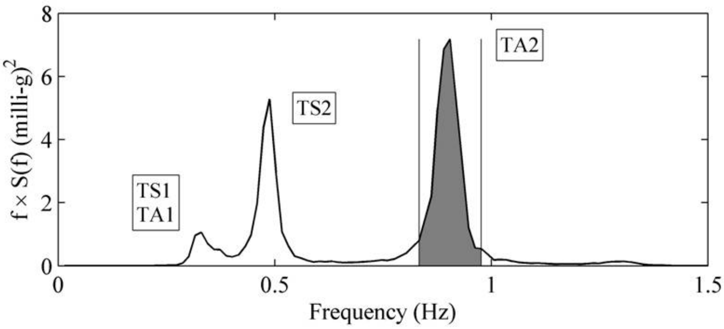

(b) Quarter Point Continuous Span

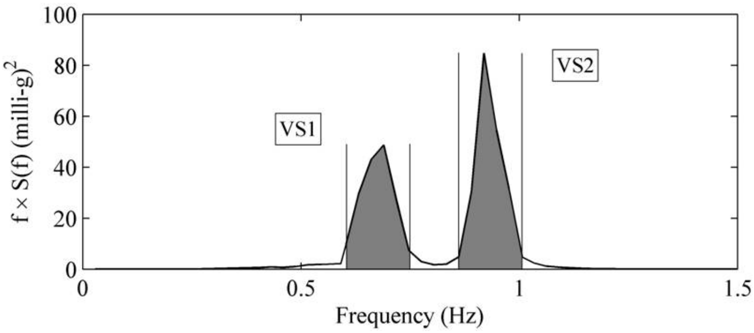

(c) Midpoint Continuous Span

Fig. 6 Power Spectra of Transverse and Vertical Accelerations

normalized acceleration independent of frequency and proportional to the normalized wind velocity on a log scale (Davenport 1988). The maximum RMS acceleration for the j^{th} mode, $a_{r_{j\max}}$, was normalized with respect to the j^{th} mode circular frequency, $\omega_j (= 2\pi f_j)$, and width of the bridge, B, to yield a normalized modal displacement, Δ_{n_j}

$$\Delta_{n_j} = \frac{a_{r_{j\max}}}{B\omega_j^2} \tag{3}$$

The associated mean wind speed, $\overline{V}$, is normalized with respect to the j^{th} mode natural frequency, f_j, and width of the bridge deck, B, to yield a reduced velocity, V^*

$$V^* = \frac{\overline{V}}{f_j B} \tag{4}$$

The relationship between the normalized variables defined in Eqs. (3) and (4) can be expressed as

$$\Delta_{n_j} = \beta (V^*)^{\alpha} \tag{5}$$

where β and α are parameters that can be obtained by regression analysis to characterize the normalized modal displacement, Δ_{n_j}, as a function of the reduced velocity, V^*. The maximum modal RMS accelerations determined in Step (ii) for the two transverse modes, TS2 and TA2, and the two vertical modes, VS1 and VS2, were normalized using Eq. (3) and the corresponding wind velocities were normalized using Eq. (4).

Figs. 7(a) and (b) show the variation of the normalized modal displacement, Δ_{n_j}, with the reduced velocity, V^*, for the transverse and vertical mode shapes, respectively. Both the horizontal and vertical axes have logarithmic scales. The solid lines have been fitted to the data for wind speeds greater than 10 m/s only, yielding

$$\Delta_{n_j} = 1.34 \times 10^{-6} (V^*)^{3.1} \tag{5a}$$

and

$$\Delta_{n_j} = 6.6 \times 10^{-6} (V^*)^{2.9} \tag{5b}$$

for the transverse and vertical modal responses, respectively. The standard errors for the exponent, parameter α in Eq. (5) are 0.053 and 0.051 and for the constant, parameter β in Eq. (5), are 5.38×10^{-8} and 1.45×10^{-7} for Eqs. (5(a) and (b)), respectively. These parameter errors indicate that, despite the scatter shown in Fig. 7, the accuracy of the estimated parameters in Eqs. (5(a) and (b)) is reasonably consistent with the precision of the values shown.

Fig. 7 shows scatter in the data for wind speeds less than 10 m/s (reduced velocity 0.92 and 1.7 for TA2 and TS2, respectively; and 0.89 and 1.23 for VS2 and VS1, respectively) so data corresponding to these low speeds were not used in fitting Eqs. (5(a) and (b)). This scatter reduces for wind speeds greater than 10 m/s but does not diminish completely, perhaps due to the presence of traffic on the bridge or the fluctuation in the turbulence intensity due to seasonal variation (King 2003). The scatter reduces for wind speeds greater than 20 m/s (V^* = 1.84 and 3.4 for TA2 and TS2, respectively, and 1.78 and 2.46 for VS2 and VS1, respectively). Although, only three data points lie in this region for each mode and the maximum wind speed observed is approximately 23 m/s (V^* = 2.12 and 3.91 for TA2 and TS2, respectively; and 2.05 and 2.83 for VS2 and VS1, respectively). The agreement between the regression fits and the data in the upper region is critical for the modal responses because the fundamental modes of vibration for long span bridges are particularly sensitive to high winds.

For the six spectral peaks identified in Fig. 6, only two transverse and two vertical peaks, shown shaded in the figures, have been used to derive Eqs. (5(a) and (b)). These equations were therefore validated for the unshaded spectral peaks (Bakht 2010). The associated RMS accelerations for the spectral peaks were within 4% of the values predicted using Eqs. (5(a) and

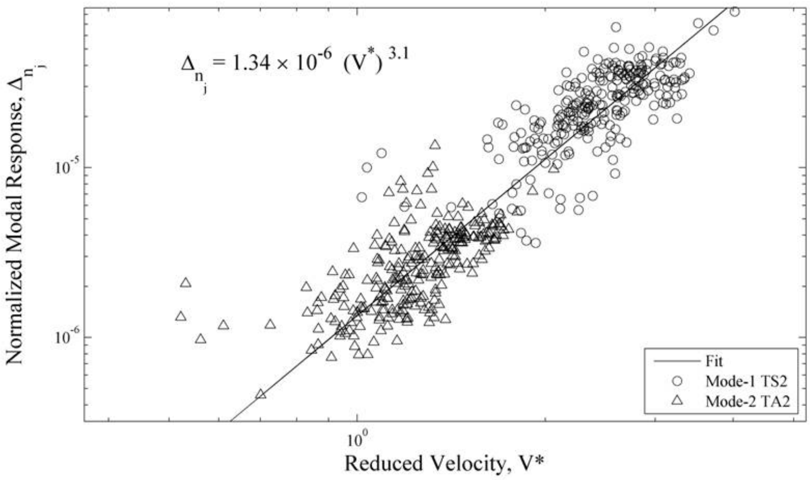

(a) Transverse

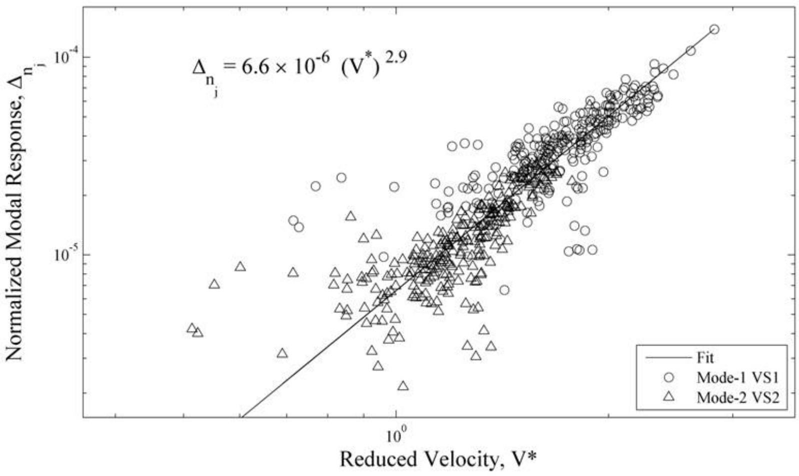

(b) Vertical

Fig. 7 Variation of Normalized Modal Displacements Ten-Minute Time History Datasets

(b)). Thus the characteristic curves given by Eqs. (5(a) and (b)) are representative of the modal responses identified from the power spectra. These curves will be used to derive the dynamic wind loads for the Confederation Bridge as described in the companion paper.

7. Damping estimates

The data gathered during the passage of Hurricane Noel in 2008 were used to estimate bridge damping using the Random Decrement Method [Cole 1973] for each mode of vibration. Table 2 summarizes the resulting damping values as percentage of critical with those reported by Londoño (2006) and Brown and Bruce (1997). The Hurricane Noel accelerometer datasets used to compute damping in the present study had an hourly mean wind speed at deck level (40.8 m) between 25

Table 2 Damping Estimates as Percentage of Critical for Different Modes of Vibration

Mode	TS1	TS2	VA1	VS1	TA2	VS2	TS3	VA2	VS3
Frequency (Hz)	0.34	0.49	0.57	0.68	0.91	0.94	1.33	1.81	2.81
Random Decrement	2.04	1.68	3.91	2.06	1.95	1.51	2.36	1.55	1.34
Londoño (2006)	1.9	1.7	3.8	2.1	2.1	1.5	0.6	1.5	1.3
Brown (1997)	-	5.7	-	-	7.7	-	5.7	-	-

and 29 m/s, which corresponds to a ten-minute mean wind speed between 26.6 and 30.9 m/s, respectively. The bridge is designed for a ten-minute mean wind speed of 30.5 m/s normal to the bridge axis at the deck elevation; therefore, it is assumed that the computed damping estimates are valid under design wind conditions. These tabulated damping values represent the total bridge damping, i.e., the sum of structural and aerodynamic damping components.

Londoño (2006) used datasets with different loading conditions, including high wind events, heavy traffic conditions and ambient traffic conditions with or without ice, to estimate damping for 25 mode shapes of the Confederation Bridge. His damping estimates are not classified based on the type of loading. Since the fundamental modes of vibration with frequencies less than 1 Hz are particularly sensitive to high winds for long span bridges, the tabulated damping estimates after Londoño, shown in Table 2, are also considered to be total bridge damping values. The values computed using the Random Decrement Method in the present study are very close to those reported by Londoño. The third transverse symmetric mode (TS3) is an exception as the value computed in the present study is 2.36% whereas Londoño predicts 0.6%. Londoño's reported value does not seem to possess both the structural and aerodynamic damping components, possibly because a traffic event caused the response used to estimate damping for this mode. Furthermore, Londoño does not report the method used to compute damping using on-site monitoring data – but he did not have access to the Hurricane Noel data, so even if his estimates are derived using the Random Decrement Method, they are based on different time histories than those used in the present study.

Brown and Bruce (1997) carried out full-scale pull tests at Pier 31 to estimate the pier stiffness using a vessel tethered by a cable to the pier. An unexpected failure of the cable provided an opportunity to collect useful data from the accelerometers and tiltmeters attached to the pier for a very large amplitude event which were subsequently used to estimate structural damping for the three transverse modes of vibration. The damping estimates by Brown and Bruce (1997), shown in Table 3.3, are higher than those reported by Londoño and higher than those determined in the present study. Brown and Bruce (1997) do not provide details of their damping calculations and so no explanation has been found to explain this difference.

8. Conclusions

The Confederation Bridge is a 43 span, 14 km long structure connecting New Brunswick and Prince Edward Island, Canada. Given the scale and unique characteristics of the structure, its owners implemented a comprehensive bridge monitoring program to capture and archive the interaction of the bridge with its environment. This paper presents the results of the analysis of a decade-long record of wind and accelerometer data to assess the accuracy of predictions made during the original design. A complete dataset of on-site monitoring wind data recorded between 1998 and 2007 was assembled and used to predict ten-minute mean wind speeds for various return periods for comparison with the original design values recommended by King *et al*. (1994). On-site monitoring accelerometer data gathered from 1998 to 2006 were analysed to determine the dynamic responses of the structure during strong wind events. These time histories were used to determine bridge natural frequencies for comparison to those computed analytically using ALGOR and reported by Londoño (2006). The fundamental mode shapes, derived using the modified beam element model in ALGOR (King *et al*. 1994, Bakht 2010), were also compared to the mode shapes estimated from full-scale data by Londoño (2006). Finally, the total damping for each mode was compared to the estimates reported by Londoño (2006) and Brown and Bruce (1997).

The following conclusions are drawn:

1. The ten-minute mean wind speed for a 100-year return period derived from the on-site bridge monitoring data collected between 1998 and 2007 is 1.5% less than the corresponding specified design wind speed predicted in 1994 and used for the bridge design.
2. The maximum ten-minute mean wind speed recorded by the on-site monitoring system between January 1998 and June 2007 is equivalent to the specified design wind speed at the deck elevation of 40.8 m and occurred on 7th November 2001. Due to its directionality and strength, it represents a near-specified design event.
3. The dynamic properties of the instrumented spans of the Confederation Bridge, i.e., natural frequencies, modes shapes and damping have been determined from the on-site monitoring data and agree well with the values reported by others. This conclusion is important for the derivation of realistic wind loads in the companion papers.
4. The dynamic bridge response shows no instabilities such as galloping, vortex shedding and flutter, which substantiate the 1994 design criteria.
5. The data from 76 accelerometers attached to the Confederation Bridge were analyzed and a significant number of the accelerometers were found to provide redundant information. Only eight strategically placed accelerometers (four transverse and four vertical) are necessary to fully quantify the dynamic response of the Confederation Bridge.

Acknowledgments

The authors would like to thank Strait Crossing Bridge Limited for providing on-site monitoring data and sponsoring scholarship applications to Natural Sciences and Engineering Research Council (NSERC) of Canada, and Mathematics of Information Technology and Complex Systems (MITACS). The generous funding through various sources including NSERC, MITACS, Western Engineering Scholarship, Western Graduate Research Scholarship, Alan G. Davenport Award and Graduate Thesis Research Awards Fund is greatly acknowledged.

References

ASCE. 7. (2005), *Minimum design loads for buildings and other structures*, American Society of Civil Engineers, Reston, Virginia, VA, USA.

Bakht, B. (2010), *Assessment of wind induced response and drivability of the Confederation Bridge,* Ph.D. Thesis, Department of Civil and Environmental Engineering, University of Western Ontario.

Brown, T.G., and Bruce, J.R. (1997), *Confederation Bridge ice force monitoring joint industry project annual report* – 1997, IFN Engineering Ltd.

Brown, T.G. (2007), "Ice force monitoring", *Confederation Bridge Engineering Summit Proceedings,* Charlottetown, PEI, Canada.

Bruce, J.R., and Croasdale, K.R. (2001), *Confederation Bridge ice force monitoring joint industry project annual report,* IFN Engineering Ltd. Report Number 00-1-001, 40p.

Cheung, M.M.S., Tadros, G.S., Brown, T., Dilger, W.H., Ghali, A. and Lau, D.T. (1997), "Field monitoring and research on performance of the Confederation Bridge", *Can. J. Civil Eng*., **24**(6), 951-962.

Cole, A.H. (1973), *On-line failure detection and damping measurement of aerospace structures by random decrement signatures,* NASA, CR-2205.

Davenport, A.G. (1964), "Note on the distribution of the largest value of a random function with application to gust loading", *Proceedings of the Institution of Civil Engineers. Paper No. 6739, Vol. 28.*

Davenport, A.G. (1977), "The prediction of risk under wind loading", *Proceedings of the 2nd International Conference on Structural Safety and Reliability – ICOSSAR,* Munich Germany pp 511-538.

Davenport, A.G. and King, J.P.C. (1984), "Dynamic wind forces on long span bridges", *Proceedings of the 12th IABSE Congress,* Vancouver, Canada.

Davenport, A.G. (1988), "The response of tension structures to turbulent wind: the role of aerodynamic damping", *Proceedings of the 1st International Oleg Kerensky Memorial Conference on Tension Structures,* London, England.

Engineering Sciences Data Units. (1993), *Strong Winds in the Atmospheric Boundary Layer,* Data Items 82026, ESDU International.

JMS. (1995), *Design Criteria Northumberland Strait Crossing Project, Revision 7.0.,* Jean Muller International, Stanley Joint Venture Inc. Calgary, Alberta.

King, J.P.C., Mikitiuk, M.J., Davenport, A.G. and Isyumov, N. (1994), *A study of wind effects for the Northumberland Straits Crossing,* BLWT-SS8-1994, Boundary Layer Wind Tunnel Laboratory, University of Western Ontario (parts of this report have been published in King and Davenport 1994, King 1999).

King, J.P.C. and Davenport, A.G. (1994), "P.E.I. fixed link – the treatment of wind effects for the northumberland strait crossing", *Proceedings of the 4th International Conference on Short and Medium Span Bridges,* Halifax, Nova Scotia, Canada.

King, J.P.C., Crooks, G.J. and Davenport, A.G. (1995), *The Northumberland Straits Crossing, Prince Edward Island Testing of Marine Span Aeroelastic Model and Analysis of Dynamic Wind Loads,* BLWT-SS24-1995, Boundary Layer Wind Tunnel Laboratory, University of Western Ontario.

King, J.P.C. (1999), "Integrating wind tunnel tests of full-aeroelastic models into the design of long span bridges", *Proceedings of the 10th International Conference on Wind Engineering (ICWE),* Copenhagen, Denmark.

King, J.P.C. (2003), *The Aerodynamics of Long Span Bridges, PhD Thesis,* Department of Civil and Environmental Engineering, University of Western Ontario, London Ontario, Canada.

Londoño, N.A. (2006), *Use of Vibration Data for Structural Health Monitoring of Bridges,* Department of Civil and Environmental Engineering, Carleton University, Ottawa, Canada.

Lau, D.T., Brown, T., Cheung, M.S. and Li, W.C. (2004), "Dynamic modeling and behaviour of the Confederation Bridge", *Can. J. Civil Eng*., **31**(2), 379-390

MacGregor, J.G., Kennedy, D.J.L., Bartlett, F.M., Chernenko, D., Maes, M.A. and Dunaszegi, L. (1997), "Design criteria and load and resistance factors for the Confederation Bridge", *Can. J. Civil Eng.,* **24**(6), 882-897.

Montreuil, M.A. (1999a), *Confederation Bridge monitoring project high-speed data logger system,* Technical Manual, Preliminary Version, Thermal Technology Centre, National Research Council Canada.

Montreuil, M.A. (1999b), *Confederation Bridge monitoring project slow-speed data logger system,* Technical Manual, Preliminary Version, Thermal Technology Centre, National Research Council Canada.

Naumoski, N., Cheung, M.S. and Foo, S. (2002), "Dynamic characteristics of the Confederation Bridge", *Can. J. Bridge Eng*., **29**, 448-458.

Naumoski, N., Cheung, M.S. and Foo, S. (2004), "Dynamic performance of the Confederation Bridge due to

traffic and wind", *Can. J. Civil Eng.*, **31**(3), 487-498.
Tadros, G. (1997), "The Confederation Bridge: an overview", *Can. J. Civil Eng.*, **24**(6), 850-866.
Xu, Z., Bekele, S., Mikitiuk, M., Isyumov, N. and Ho, E. (2008), "Bi-Modal weibull distribution fit for climatic wind speed histogram", *Proceedings of the 13th Australian Wind Engineering Society (AWES) Workshop,* Hobart, Australia.

CC